Natural Hazards (2023) 117:365–380
https://doi.org/10.1007/s11069-023-05863-9

ORIGINAL PAPER

Regression relationships for conversion of body wave and surface wave magnitudes toward Das magnitude scale, M_{wg}

Ranjit Das[1,2] · Claudio Menesis[1] · Diego Urrutia[1]

Received: 22 March 2022 / Accepted: 7 February 2023 / Published online: 15 March 2023

Abstract
A reliable and standardized estimation of earthquake size is a fundamental requirement for all tectonophysical and engineering applications. Several investigations raised questions about the determinations of smaller and intermediate earthquakes using M_w scale. Recent investigations (Das et al. in Bull Seismol Soc Am 108(4):1995–2007, 2018b) show that the moment magnitude scale M_w is not applicable for lower and intermediate ranges throughout the world and does not efficiently represent the seismic source potential due to its dependence on surface wave magnitudes; therefore, an observed seismic moment (M_0)-based magnitude scale, M_{wg}, which smoothly connects seismic source processes and highly correlates with seismic-radiated energy (E_s) compared to the M_w scale is suggested. With the goal of constructing a homogeneous data set of M_{wg} to be used for earthquake-related studies, relationships for body wave (m_b) and surface wave magnitudes (M_s) toward M_{wg} have been developed using regression methodologies such as generalized orthogonal regression (GOR) (GOR1: GOR relation is expressed in terms of the observed independent variable; and GOR2: GOR relation is used inappropriately in terms of theoretical true point of GOR line) and standard least-square regression (SLR). In order to establish regression relationships, global data have been considered during 1976–2014 for m_b magnitudes of 524,790 events from the International Seismological Centre (ISC) and 326,201 events from the National Earthquake Information Center (NEIC), M_s magnitudes of 111,443 events from ISC along with 41,810 M_{wg} events data from the Global Centroid Moment Tensor (GCMT). Scaling relationships have been obtained between m_b and M_{wg} for magnitude range $4.5 \le m_b \le 6.2$ for ISC and NEIC events using GOR1, GOR2 and SLR methodologies. Furthermore, scaling relationships between M_s and M_{wg} have been obtained for magnitude ranges $3.0 \le M_s \le 6.1$ and $6.2 \le M_s \le 8.4$ using GOR1, GOR2 and SLR procedures. Our analysis found that GOR1 provides improved estimates of dependent variable compared to GOR2 and SLR on the basis of statistical parameters (mainly uncertainty on slope and intercept, RMSE and Rxy) as reported in Das et al. (2018b). The derived global scaling relationships would be helpful for various seismological applications such as seismicity, seismic hazard and Risk assessment studies.

Keywords Earthquake catalog · Orthogonal regression · Seismic hazard

Extended author information available on the last page of the article

1 Introduction

The earthquake magnitude scale is one of the most fundamental earthquake source parameters used for measuring the strength of an earthquake. In 1935, the first earthquake magnitude scale (local magnitude: M_L) was introduced by Richter (1935) for earthquakes in Southern California. After 10 years, Gutenberg (1945a) extended the local magnitude scale to measure earthquakes at long distances and defined the earthquake magnitude scale as "M_s" called the surface-wave magnitude, considering the surface wave (period between 17 and 23 s) of a seismic signal.

The concept of body wave magnitude was first proposed by Gutenberg (1945a, b) and later redefined by Gutenberg and Richter (1956). Long period body wave magnitude (mB) determination is based on the ratio of maximum amplitude to period of P or S waves with periods up to about 10 s recorded by intermediate- to long-period instruments (Das et al. 2011). The body wave magnitude (m_b) is determined using P waves around 1 s, and time periods considered for mB are several to 10 s. (Das et al. 2011). The surface wave magnitude scale does not work for higher earthquake size because of saturation. The saturation of surface wave magnitude occurs when fault rupture dimension of an earthquake exceeds the wavelength of the earthquake wave used for magnitude estimation.

Kanamori (1977) and Hanks and Kanamori (1979) developed another scale called M_w scale that is often considered as non-saturating magnitude scale. M_w scale is mainly developed on the following issues: (1) M_w scale is only adequate for larger earthquake (Kanamori 1977); (2) The validation step of the development of M_w scale is solely performed on Southern Californian Seismicity (Tables 1 and Table 2 of Hanks and Kanamori 1979); thus, applicability of M_w scale ≥ 3.0 is only valid for Southern California not for worldwide. (3) M_w scale is based on the relationship between Energy and Surface wave magnitude, and thus, it is not closely related with source; (4) Direct observed seismic moment record is not considered in the development of M_w scale only based on substitution; (5) M_w scale used constant stress drop which is applicable for upper crust; therefore, applicability of M_w scale is also limited to the upper crust.

Despite the popularity of M_w, it provides limited information about the earthquake source, especially regarding its high-frequency content (e.g., Beresnev 2009) which is more relevant for the evaluation of an earthquake's shaking potential. It has also been observed by many authors that using only one scale, i.e., M_w scale does not serve the purpose for measuring the actual size of earthquakes due to its inherent limitations (e.g., Kanamori 1977; Choy and Boatwright 1995; Kanamori and Brodsky 2004; Bormann et al. 2009; Wason et al. 2012; Das 2013; Das et al. 2013, 2014b, 2018b, Lin et al. 2020).

Recently, an advanced unsaturated earthquake magnitude scale, i.e., Das magnitude scale M_{wg}, has been reported (Das et al. 2019) which circumvents the limitations of M_w scale. The M_{wg} scale is mainly based on observed seismic moment record using worldwide data. The M_{wg} is based on low- and high-frequency spectra of seismic signal. The M_{wg} scale is well connected with radiated energy and observed magnitude scales (e.g., m_b, M_s, M_e). M_{wg} scale is directly proportional to the logarithm of the observed seismic moment, and thus, it is related to seismic source process, and it is not saturated for large magnitude earthquakes. Therefore, M_{wg} scale depicts a uniform behavior for wider magnitude ranges. Thus, it is preferred to compile earthquake catalogs with all magnitudes expressed in this unified scale M_{wg} for the purpose of seismic hazard assessment and other important seismological studies associated with seismicity.

Toward preparation of a homogeneous earthquake catalog, it is generally required to express different magnitudes as one magnitude (M_{wg}) using regression relationships. We provide regression relationships of entire world for body and surface wave magnitudes toward seismic moment scale M_{wg} using SLR (Standard Least-square Regression), GOR2 (General orthogonal Regression: suggested in Fuller 1987 and Carroll and Ruppert 1996) and GOR1(General Orthogonal Regression suggested in Das et al. 2018b) as suggested in recent literature (Das et al. 2011, 2016; Das et al. 2014a, b, 2018a; Fuller 1987; Nath et al. 2017; Ristau 2009; Wason et al. 2012).

2 Seismic moment magnitude (M_{wg}) and moment magnitude (M_w) scales

To understand the magnitude scales based on M_o detailed background of M_{wg} and M_w scales is given below.

2.1 M_w scale

Kanamori (1977) defined a magnitude scale (Log $W_0 = 1.5\ M_w + 11.8$, where W_0 is the minimum strain energy) for great earthquakes using Gutenberg Richter Eq. (1).

$$\text{Log } E_s = 1.5M_s + 11.8. \tag{1}$$

Kanamori (1977) used W_0 in place of E_s (dyn.cm) and consider a constant term ($W_0/M_o = 5 \times 10^{-5}$) in Eq. (1) and estimated M_s and denoted as M_w (dyn.cm). It is important to note that the energy Eq. (1) is derived by substituting $m = 2.5 + 0.63$ M in the energy equation Log $E = 5.8 + 2.4$ m (Richter 1958), where m is the Gutenberg unified magnitude and M is a least squares approximation to the magnitude determined from surface wave magnitudes. After replacing the ratio of seismic Energy (E) and Seismic Moment (M_o), i.e., $E/M_o = 5 \times 10^{-5}$, into the Gutenberg–Richter energy magnitude Eq. (1), Hanks and Kanamori (1979) provided Eq. (2):

$$\text{Log } M_o = 1.5M_s + 16.1 \tag{2}$$

Note that Eq. (2) was already derived by Kanamori (1977) and termed it as M_w. Eq. (2) was based on large earthquakes; hence, in order to validate Eq. (2) for intermediate and smaller earthquakes, Hanks and Kanamori (1979) compared this Eq. (2) with Eq. (1) of Percaru and Berckhemer (1978) for the magnitude $5.0 \le M_s \le 7.5$ (Hanks and Kanamori 1979). Note that Eq. (1) of Percaru and Berckhemer (1978) for the magnitude range $5.0 \le M_s \le 7.5$ is not reliable due to the inconsistency of defined magnitude range (moderate to large earthquakes defined as $M_s \le 7.0$ and $M_s = 7$–7.5) and scarce data in lower magnitude range (≤ 7.0) which rarely represents the global seismicity (e.g., see Figs. 1A, B, 4 and Table 2 of Percaru and Berckhemer 1978).

In order to validate Eq. (2) for the lower magnitude range, Eq. (2) is compared with the Sothern California M_o and M_L relationship for the magnitude range $3.0 \le M_L \le 7.0$. It is natural that the relationship between M_0 and M_L will vary due to different seismotectonic and geological setting (e.g., Hutton and Boore 1987; Choy and Boatwright 1995; Ristau et al. 2003; Keir et al. 2006). As stated above and in earlier studies (e.g., Das et al. 2019), validation of M_w scale was performed on Californian seismicity; therefore, the M_w scale

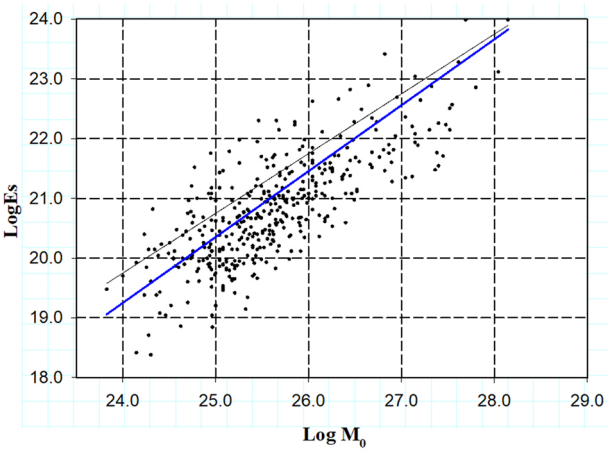

Fig. 1 Radiated energy (E_s) of the global data set plotted as a function of seismic moment. The radiated energy values are predicted using M_w (Black solid line) and M_{wg} (Blue solid line). Most of the earthquakes using M_w overestimate the actual radiated energy (Das et al. 2019)

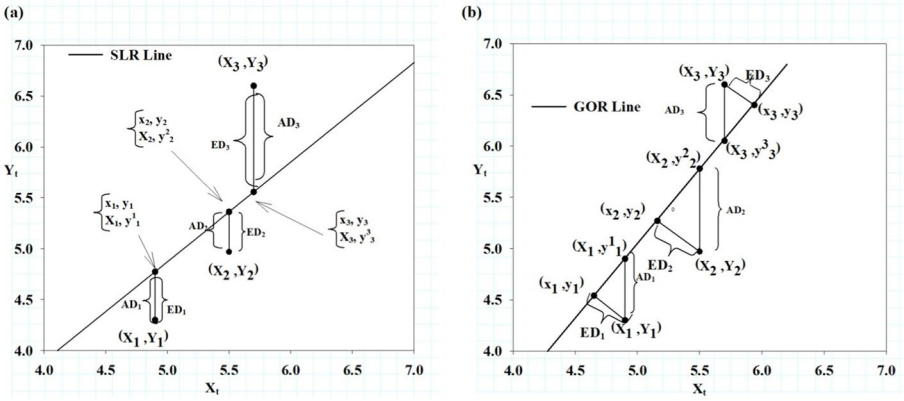

Fig. 2 Schematic diagram showing theoretical true points (i.e., (x_t, y_t), $t=1, 2, 3$) and estimated points (i.e., (X_t, Y^*_t), $t=1, 2, 3$) on the fitted regression line (solid black line) for a set of three observed points (X_1, Y_1), (X_2, Y_2), and (X_3, Y_3); **a** standard linear-square regression (SLR) line; **b** general orthogonal regression (GOR) line

(2/3 log M_o−10.7) provided by Hanks and Kanamori (1979) is only applicable for certain region. Hanks and Kanamori (1979) also referred to their formulation that M_w is uniformly valid for $M_w \geq 7.5$ as pointed out by Kanamori (1977). Therefore, its use worldwide is not appropriate for magnitude ranges < 7.5. This can also be easily understood from the strong deviations of M_w with m_b and M_s scales (Figs. 1, 2 and 3 of Das et al. 2019). It is important to note that the comparison between M_w scale and observed other magnitude scales (M_L and M_s) was the main criteria for validation of M_w scale in Hanks and Kanamori (1979). This type of comparison (observed Vs estimated) used in the validation of M_w scale is the standard practice of Seismological study as well as in other literature (e.g., Ekstrom and Dziewonski 1988). The reason of disagreement for smaller and intermediate magnitude ranges between M_w scale and different observed magnitude scales (m_b, M_s and M_c) is due to the unavailability of smaller and intermediate earthquakes (or very limited intermediate earthquakes) in the relationship (Log $M_o = 1.5M_s + 16.1$) that was used for the formulation of M_w scale. The derivation of M_w scale involves a constant term stress drop ($\Delta\sigma$) which

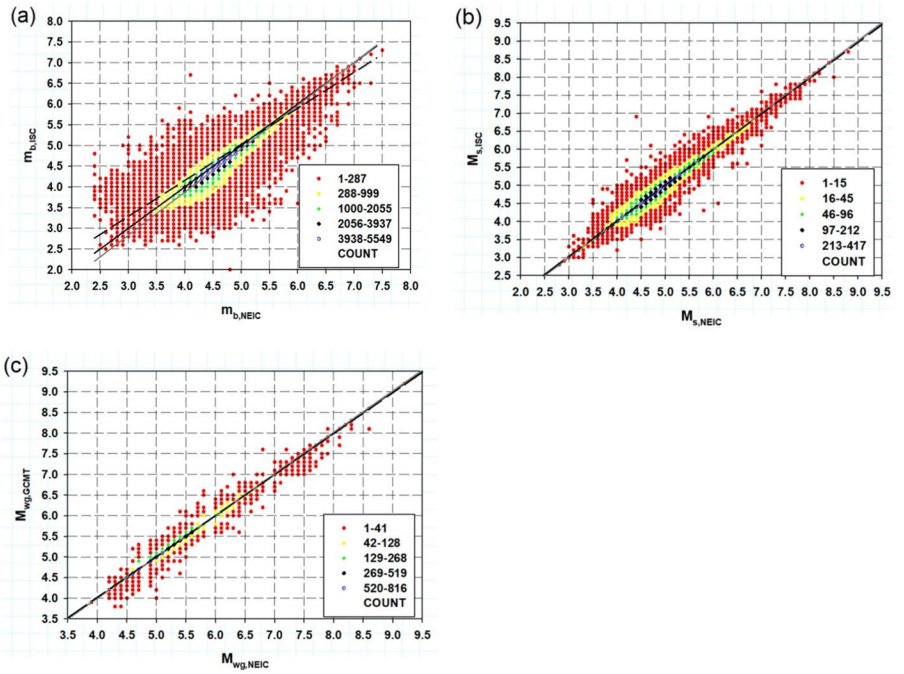

Fig. 3 Correlations of magnitude scales. Plots of regression relations using GOR1 (black solid line), GOR2 (gray solid line) and SLR (black dashed line): **a** $m_{b,ISC}$ vs $m_{b,NEIC}$, **b** between $M_{s,ISC}$ vs $M_{s,\ NEIC}$, **c** $M_{wg,\ GCMT}$ vs $M_{wg,\ NEIC}$

varies generally from few bars to 125. The variability of $\Delta\sigma$ is significant; therefore, stress drop cannot be assumed to be constant (See Table 2, Percaru and Berckhemer 1978). Hence, depending on the value of constancy, M_w value for a given earthquake will change significantly. Furthermore, the value of constancy (E_s/M_o) in the derivation of M_w scale is only applicable for shallow earthquakes. Thus, M_w scale is only applicable for shallow earthquakes mainly for two reasons: (1) M_w scales are primarily derived from surface wave scale because the fundamental equation used for obtaining the M_w scale was a relationship between Energy and Surface wave magnitude (Log $E_S = 1.5M_s + 11.8$), and (2) Used constant value ($E_s/M_o = 5*10^{-5} = \frac{\Delta\sigma}{2\mu}$) in the development of M_w scale is only applicable for shallow earthquakes. The unsaturated M_w is globally valid for large earthquake as M_w scale was based on equations Log $E_S = 1.5M_s + 11.8$ and Log $M_0 = 1.5M_s + 16.1$ (Details are given in Richter 1958; Kanamori 1977; Purcaru and Berckhemer 1978).

2.2 M_{wg} scale (Das magnitude scale)

In order to develop advanced seismic moment magnitude scale (M_{wg}), Das et al. (2019) collected a total of 25,708 directly observed seismic moment values, along with m_b magnitudes representing global seismicity, which were compiled from Global Centroid Moment Tensor (CMT) and International Seismological Centre (ISC) databases, respectively, for the time period 1976–2006. To validate the M_{wg} scale, 18,521 Ms events and energy

magnitudes with 1316 events have been collected from ISC, NEIC, respectively. Furthermore, 397 seismic-radiated energy data have been collected from Choy and Boatwright (1995).

Das et al. (2019) derived simple least-squares fitting relationship between M_0 and m_b using 25,708 global events, which is as follows:

$$\text{Log } M_0 = 1.36m_b + 17.24. \tag{3}$$

As discussed above, M_w scale was developed from the equation Log $E_S = 1.5M_s + 11.8$. In this equation, M_s is saturated around 8.6; thus, applicability of M_w is valid up to 8.6. But, if E_s is known independently and put in this equation, then M_s would not saturate (Hanks and Kanamori 1979). In Eq. (3), M_0 knows independently; therefore, substituting M_o in left-hand side of Eq. (3) will produce M_{wg} and it will not saturate, as given in Eq. (4).

$$M_{wg} = \frac{\text{Log } M_o}{1.36} - 12.68 \tag{4}$$

Both M_w and M_{wg} are in terms of M_o (dyn cm), so they are physics based and will not saturate. One can easily estimate M_o from M_w scale by using Eq. (5)

$$\text{Log } M_o = \frac{3 \times \left(M_w + 10.7\right)}{2} \tag{5}$$

Tohoku-Oki earthquake (March 11th, 2011) has an M_w value of 9.1 and caused serious damage. Using Eq. (5), Log M_o of Tohoku-Oki earthquake will be 29.72509452, and then, using Eq. (4) one can estimate M_{wg} as 9.2.

The M_{wg} scale is highly correlated with radiated energy E_s (Fig. 1) and observed magnitudes (e.g., m_b, M_s, M_e) as reported in Das et al. (2019).

3 Methodology

General orthogonal regression (GOR) yields a linear relationship between dependent (y_t) and independent (x_t) variables based on observed data (X_t, Y_t) having errors in both the variables (Madansky 1959; Kendall and Stuart 1979; Das et al. 2018b). In the conventional GOR (GOR2) procedure, estimate of y_t is obtained by substituting X_t (instead of x_t) in the GOR relation ($y_t = \beta_0 + \beta_1 x_t$). The conventional procedure produces a bias in the estimate as demonstrated in recent publications (e.g., Wason et al. 2012; Das et al. 2014a, b, 2018a). Hence, this problem was corrected by adding one additional step in the estimation procedure as explained in Wason et al.(2012) and Das et al. (2018b) and thus, the application of GOR2 must include the suggested correction to overcome the limitations of GOR2 (see Wason et al. 2012; Das et al. 2014a,b, 2018a, b). Carroll and Ruppert (1996) had also reported about the misuse of GOR2 and cautioned for the over estimation of regression slope. The difference between Carroll and Ruppert (1996) and Das et al. (2018b) is that Das et al. (2018b) used error variance value given by Fuller (1987), but Carroll and Ruppert (1996) modified the error variance value (η) to adjust the overestimation of slope. Das et al. (2018b) adjusted the overestimation of slope through an intermediate step in which GOR is corrected. The corrected GOR as described in Das et al. (2018b) is henceforth denoted as GOR1. In order to better understand the limitations of GOR, a graphical

representation of GOR has been discussed below. The methodology GOR2 is called as OR (Orthogonal Regression) when η is considered to be 1.

3.1 A graphical representation of GOR

The graphical representation of GOR is provided below for easy understanding the limitations involved in the GOR method. It is observed that GOR inherent problem is not well addressed in the existing literature before the study of Das et al. (2012); therefore, to provide a clear view on GOR, two different cases are discussed below.

3.1.1 Case I

Let us consider a SLR line obtained from data pairs (X_1, Y_1), (X_2, Y_2) and (X_3, Y_3), and the corresponding theoretical true points on the SLR line are $(x_1 = X_1, y_1)$, $(x_2 = X_2, y_2)$ and $(x_3 = X_3, y_3)$, respectively. Note that these theoretical true points on the line are used to derive the best fitting SLR line by minimizing the vertical residuals. On substituting the independent observed variables X_1, X_2, X_3 in the obtained SLR line, one can achieve the theoretical true points $((x_1 = X_1, y_1)$, $(x_2 = X_2, y_2)$ and $(x_3 = X_3, y_3))$ that were used in the derivation of the best fitting SLR line. In Fig. 2a, ED_1, ED_2 and ED_3 are the Euclidean distances between (X_1, Y_1) and $(x_1 = X_1, y_1)$, (X_2, Y_2) and $(x_2 = X_2, y_2)$, and (X_3, Y_3) and $(x_3 = X_3, y_3)$, respectively. These Euclidean distances are used during the development of the SLR line.

Let AD_1, AD_2, AD_3 be the achievable distances after substitution of X_1, X_2, X_3 in the obtained SLR relation**.** Note that in SLR, distances used during minimization for building the line can also be achieved in the estimations, i.e., $ED1 = AD_1$, $ED_2 = AD_2$, $ED_3 = AD_3$ (Fig. 2a).

3.1.2 Case II

Consider a GOR line obtained using observed data pairs (X_1, Y_1), (X_2, Y_2), and (X_3, Y_3), with errors in both the variables. The theoretical true points (true Points) of these data pairs on the GOR line, i.e., (x_1, y_1), (x_2, y_2) and (x_3, y_3) are given by minimizing the Euclidean distance (statistical Euclidean distance or weighted orthogonal distance). By substituting observed values X_1, X_2, X_3 in the obtained GOR line, the corresponding theoretical true points cannot be achieved unlike in the Case I. Instead of obtaining the theoretical true points, totally different points on the GOR line are achieved (see Fig. 2b). This issue can also be understood using Euclidean distance concept.

Let the used Euclidean distances during the development of GOR line be ED_1, ED_2, ED_3 between the data points (X_1, Y_1) and $(x_1 = X_1, y_1)$, (X_2, Y_2) and $(x_2 = X_2, y_2)$, and (X_3, Y_3) and $(x_3 = X_3, y_3)$, respectively. It is important to note that the achievable distances (i.e., AD_1, AD_2, AD_3), after substitution of independent variables (i.e., X_1, X_2, X_3) in the GOR line, are not the same with Euclidean distances (i.e., ED_1, ED_2, ED_3), e.g., $AD_1 \neq ED_1$, $AD_2 \neq ED_2$, and $AD_2 \neq ED_3$, however, these distances remain the same for SLR in case I: $AD_1 = ED_1$, $AD_2 = ED_2$, $AD_3 = ED_3$.

Hence, GOR2 introduced bias in the estimation as it is not possible to get the corresponding true point on the direct substitution of any observed value of the independent variable in the GOR line. Therefore, the Squared Euclidean distance (Fuller 1987, F1.3.14) is not applicable in case of GOR.

3.2 Conversion relationships among different magnitude scales

The GOR relationship requires error variance ratio values (η) for its derivation. To find the uncertainties associated with m_b, M_s and M_{wg} magnitude determinations, standard deviation of the differences between the magnitude determinations by two different agencies for a same type of earthquake magnitude have been estimated. In the case of m_b or M_s, the standard deviations have been estimated from the differences between observed ISC and NEIC data, and for M_{wg}, differences have been obtained between observed GCMT and NEIC data. The comparative standard deviations associated with different magnitude types are estimated to be 0.09, 0.11, 0.12 and 0.2 for M_{wg}, M_w, M_s and m_b, respectively. These values are consistent with other reported values suggested in earlier studies (e.g., Kagan 2003; Das et al. 2011). The knowledge of error variance ratio (η) is very critical for performing GOR relations. The use of equation error in estimating η has not addressed in GOR equations performed in earlier seismological studies, except in Das et al. (2018b). Carroll and Ruppert (1996) suggested to use $\eta = \frac{\sigma_e + \sigma_q}{\sigma_u}$ (where σ_q, denotes equation error, see Table 1 of Carroll and Ruppert 1996) instead of using $\eta(\eta = \frac{\sigma_e}{\sigma_u})$ because equation error σ_q, is not considered. As equation error calculation is not straight forward, therefore, we use Fuller (1987) method of estimating $\eta = \frac{\sigma_e}{\sigma_u}$ and equation error σ_q, has been encountered through an intermediate extra step employed in GOR1.

For m_b to M_w conversion, we used $\eta = \frac{\sigma_e}{\sigma_u} = \frac{0.09 \times 0.09}{0.2 \times 0.2} = 0.2$, and for M_s to M_{wg} we used $\eta = \frac{\sigma_e}{\sigma_u} = \frac{0.09 \times 0.09}{0.12 \times 0.12}. = 0.56$. The regression relationships (i.e., GOR1, GOR2) among different agencies (e.g., ISC vs NEIC and GCMT vs. NEIC) for different magnitude scales (i.e., m_b, M_s) with $\eta = 1$ are shown in Fig. 3.

Out of all, 245,899 events have m_b values both from ISC and NEIC. The GOR1, GOR2 and SLR relationships with $\eta = 1$ between $m_{b,\,ISC}$ and $m_{b,\,NEIC}$ are as given below (Fig. 3).

$$m_{b,ISC} = 0.990(\pm 0.001) mb_{,NEIC} - 0.052(\pm 0.002),\ \text{RMSE} = 0.114,\ R_{xy} = 0.974 \quad (6)$$

$$m_{b,ISC} = 1.043(\pm 0.009) mb_{,NEIC} + 0.297(\pm 0.004),\ \text{RMSE} = 0.224, R_{xy} = 0.90 \quad (7)$$

$$m_{b,ISC} = 0.940(\pm 0.002) mb_{,NEIC} + 0.174(\pm 0.004),\ \text{RMSE} = 0.219,\ R_{xy} = 0.94 \quad (8)$$

The developed corresponding relationships between $M_{s,\,ISC}$ and $M_{s,\,NEIC}$ are as follows (Fig. 3)

$$M_{s,ISC} = 0.988(\pm 0.001) M_{s,NEIC} + 0.065(\pm 0.005),\ \text{RMSE} = 0.085,\ R_{xy} = 0.99 \quad (9)$$

$$M_{s,ISC} = 1.001(\pm 0.002) M_{s,NEIC} - 0.002(\pm 0.01),\ \text{RMSE} = 0.171,\ R_{xy} = 0.98 \quad (10)$$

$$M_{s,ISC} = 0.974(\pm 0.002) M_{s,NEIC} + 0.131(\pm 0.009),\ \text{RMSE} = 0.17,\ R_{xy} = 0.95 \quad (11)$$

The GOR1, GOR2 and SLR relationships with $\eta = 1$ between $M_{wg,\,GCMT}$ and $M_{wg,\,NEIC}$. are as given below (Fig. 3).

$$M_{wg,GCMT} = 0.997(\pm 0.001) M_{wg,NEIC} + 0.025(\pm 0.003),\ \text{RMSE} = 0.049,\ R_{xy} = 0.99 \quad (12)$$

$$M_{\mathrm{wg,GCMT}} = 1.003(\pm 0.002)M_{\mathrm{wg,NEIC}} - 0.008(\pm 0.008),\ \mathrm{RMSE} = 0.098,\ R_{\mathrm{xy}} = 0.99 \tag{13}$$

$$M_{\mathrm{wg,GCMT}} = 0.991(\pm 0.001)M_{\mathrm{wg,NEIC}} + 0.058(\pm 0.01),\ \mathrm{RMSE} = 0.097, R_{\mathrm{xy}} = 0.98 \tag{14}$$

3.3 Body wave magnitude to seismic moment magnitude (M_{wg})

Body wave magnitudes for 5, 24,790 of ISC and 3,26,106 of NEIC have been considered during the period 01 January 1976–31 December 2014. GOR1, GOR2 and SLR relations have been derived between $m_{\mathrm{b,ISC}}$ and $M_{\mathrm{wg,\ GCMT}}$ considering 36,767 events for the magnitude range $4.5 \leq m_{\mathrm{b,ISC}} \leq 6.2$ for different η values. The slope and intercept coefficients of the relationships for different η values are shown in Fig. 4a, and GOR1, GOR2 and SLR relationships between m_{b} and M_{wg} using $\eta = 0.2$ are given in Eqs. 15, 16, 17, respectively.

$$GOR1:\ M_{\mathrm{wg}} = 0.929(\pm 0.003)mb_{,\mathrm{ISC}} + 0.261(\pm 0.019),\ \mathrm{RMSE} = 0.25,\ R_{\mathrm{xy}} = 0.79 \tag{15}$$

$$GOR2:\ M_{\mathrm{wg}} = 1.508(\pm 0.007)mb_{,\mathrm{ISC}} - 2.726(\pm 0.036),\ \mathrm{RMSE} = 0.39,\ R_{\mathrm{xy}} = 0.52 \tag{16}$$

$$SLR:\ M_{\mathrm{wg}} = 0.879(\pm 0.004)mb_{,\mathrm{ISC}} + 0.524(\pm 0.022),\ \mathrm{RMSE} = 0.28,\ R_{\mathrm{xy}} = 0.74 \tag{17}$$

The plots of above relationships (Eqs. 15–17) for $\eta = 0.2$ are shown in Fig. 5. It has been observed from Fig. 5 that GOR1 relationships lie in the middle in the majority of magnitude ranges; however, GOR2 line does not follow the same pattern. GOR1 line passes between SLR and GOR2. It has been observed from Eqs. 15–17 that the

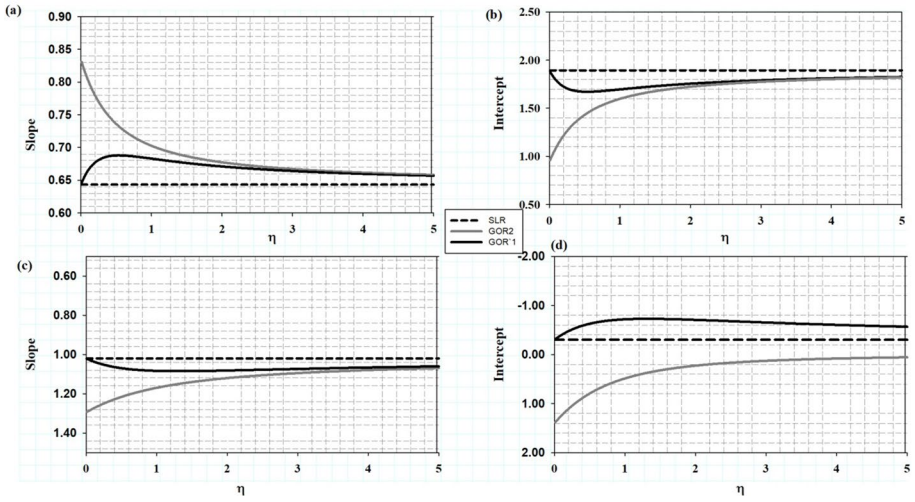

Fig. 4 Variations of slope and intercept parameters with respect to η for GOR1 (black solid line), GOR2 (gray solid line) and SLR (black dashed line) relations: **a**, **b** Relationship between $m_{\mathrm{b,ISC}}$ and M_{wg} **c**, **d** Relationship between $m_{\mathrm{b,NEIC}}$ and M_{wg}

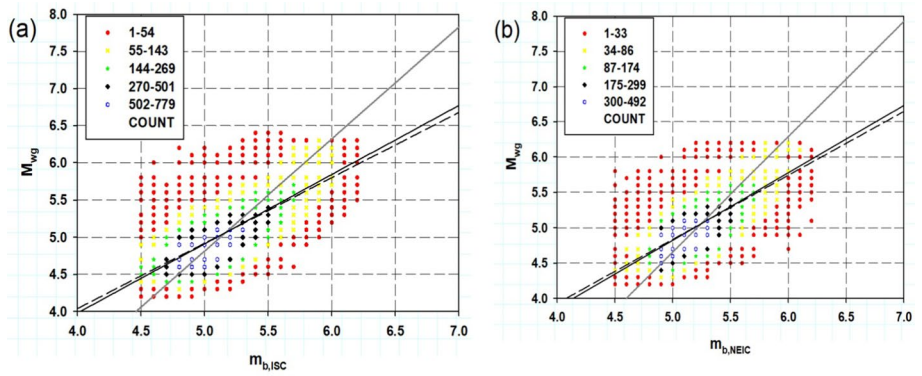

Fig. 5 Plots of regression relations using GOR1 (black solid line), GOR2 (gray solid line) and SLR (black dashed line): **a** between $m_{b,ISC}$ and M_{wg}, **b** between $m_{b,NEIC}$ and M_{wg}

uncertainty values in slope and intercept obtained though GOR1 have significant improvement over SLR and GOR2.

Furthermore, GOR1, GOR2 and SLR relationships have been derived between $m_{b,NEIC}$ and $M_{wg,\,GCMT}$ for the magnitude range $4.5 \le m_{b,NEIC} \le 6.2$ for different η values. The variations of slope and intercept coefficients with respect to η values are shown in Fig. 4, and the GOR1, GOR2 and SLR relationships between body wave magnitude of NEIC and seismic moment magnitudes for $\eta = 0.2$ are given as follows:

$$M_{wg} = 0.956(\pm 0.006)mb_{,NEIC} + 0.045(\pm 0.029),\ \text{RMSE} = 0.25,\ R_{xy} = 0.76 \quad (18)$$

$$M_{wg} = 1.635(\pm 0.01)mb_{,NEIC} - 03.516(\pm 0.055),\ \text{RMSE} = 0.36,\ R_{xy} = 0.5 \quad (19)$$

$$M_{wg} = 0.905(\pm 0.007)mb_{,NEIC} + 0.311(\pm 0.032),\ \text{RMSE} = 0.28,\ R_{xy} = 0.72 \quad (20)$$

The plots of the all regression relationships (Eqs. 18–20) are shown in Fig. 5. In conversion from $m_{b,NEIC}$ to M_{wg}, GOR1 provides estimates closer to SLR, but have lower uncertainties in slope and intercept along with standard deviations and correlation coefficients compared to GOR2 and SLR.

3.4 Surface wave magnitudes to seismic moment magnitudes

It has been found that the 21,474 global M_s events used in this study for magnitude range $3.1 \le M_s \le 8.4$ depict a bilinear trend the same was also suggested by Wason et al. (2012). Hence, the magnitude range has been subdivided into two parts, that is, $3.1 \le M_s \le 6.1$ and $6.2 \le M_s \le 8.4$, assuming that the distribution is linear in these respective magnitude ranges (Fig. 6a).

In order to convert M_s to M_{wg}, 19, 826 events have been considered in the magnitude range $3.1 \le M_s \le 6.1$ and 1639 events in the magnitude range $6.2 \le M_s \le 8.4$. GOR1, GOR2 and SLR relationships between M_s and M_{wg} with $\eta = 0.56$ for the magnitude range $3.1 \le M_s \le 6.1$ are given below.

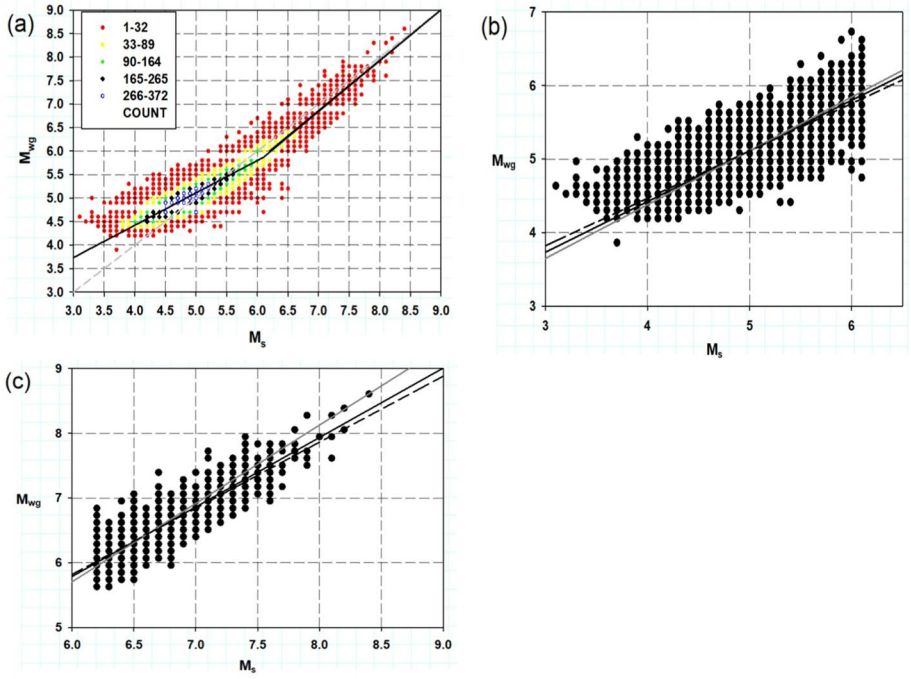

Fig. 6 Plots of regression relations using GOR1 (black solid line), GOR2 (gray solid line) and SLR (black dashed line): **a** A merged plot of M_s and M_{wg} data pairs presenting the bilinear trend, **b** between M_s Vs M_{wg} in the range $3.1 \leq M_s \leq 6.1$, **c** M_s vs M_{wg} in the range $6.2 \leq M_s \leq 8.4$

$$M_{wg} = 0.688(\pm 0.001)M_s + 1.672(\pm 0.006),\ \text{RMSE} = 0.09,\ R_{xy} = 0.97 \tag{21}$$

$$M_{wg} = 0.730(\pm 0.003)M_s + 1.459(\pm 0.014),\ \text{RMSE} = 0.09,\ R_{xy} = 0.87 \tag{22}$$

$$M_{wg} = 0.643(\pm 0.002)M_s + 1.894(\pm 0.012),\ \text{RMSE} = 0.188,\ R_{xy} = 0.88 \tag{23}$$

The developed corresponding relations for $6.2 \leq M_s \leq 8.4$ are as follows:

$$M_{wg} = 1.073(\pm 0.009)M_s - 0.646(\pm 0.062),\ \text{RMSE} = 0.147,\ R_{xy} = 0.94 \tag{24}$$

$$M_{wg} = 1.209(\pm 0.005)M_s - 1.549(\pm 0.09),\ \text{RMSE} = 0.23,\ R_{xy} = 0.91 \tag{25}$$

$$M_{wg} = 1.02(\pm 0.013)M_s - 0.301(\pm 0.806),\ \text{RMSE} = 0.24,\ R_{xy} = 0.93 \tag{26}$$

The plots of regression relationships from Eqs. 21–26 are shown in Fig. 6. It is observed from Fig. 6 that GOR1 lies in the middle between GOR2 and SLR. GOR2 shows overestimation values in almost all the ranges of Fig. 6c, and SLR shows underestimation values in the majority portion of both the magnitude ranges of M_s. The variations of slope and intercept values with respect to η are shown in Fig. 7. It has been observed from Fig. 7 that for $\eta > 3.5$, both the GOR2 and GOR1 show nearly equivalent results.

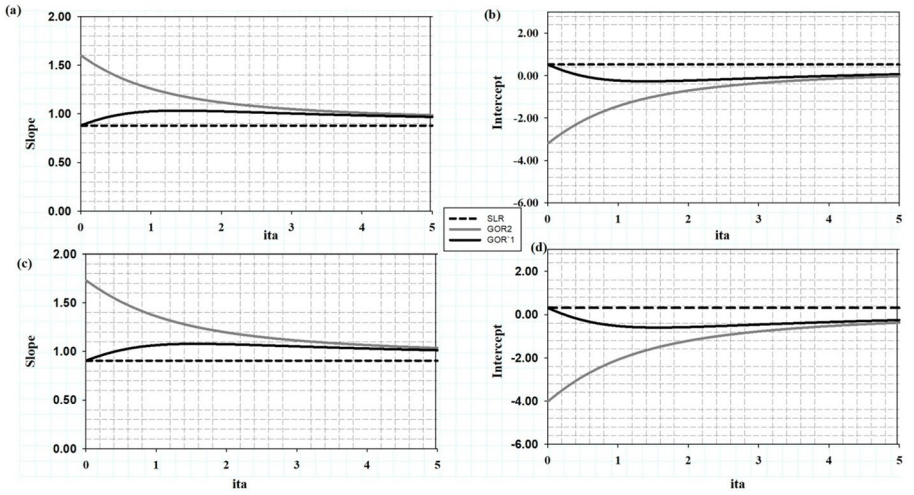

Fig. 7 Variations of slope and intercept coefficients with respect to η for GOR1 (black solid line), GOR2 (gray solid line) and SLR (black dashed line) relations: **a**, **b** Relationship between M_s and M_{wg} in the magnitude range $3.1 \leq M_s \leq 6.1$. **c**, **d** Relationship between M_s and M_{wg} for the magnitude range $6.2 \leq M_s \leq 8.4$

4 Discussions and conclusions

The M_{wg} is an unsaturated magnitude scale, based on both low-and high-frequency spectra of a seismic signal using observed M_o, connects smoothly the seismic source potential and seismic-radiated energy and is applicable for wider magnitude ranges (>3.5) worldwide. Existing low-frequency spectra based M_w are only applicable for ≥ 7.5 worldwide (Kanamori 1977, Table 1 and Table 2 of Hanks and Kanamori 1979; Das et al. 2019). The use of M_w scale for ≥ 3.0 is only applicable for Southern California; however, each part of entire globe has different tectonic environment and geological setting; therefore, use of M_w scale for ≥ 3.0 in entire globe will have adverse effects on Seismicity, Earthquake Hazard Assessment, Early Warning System, and other related seismological studies.

Therefore, a uniform earthquake catalog in terms of M_{wg} applicable for lower, intermediate and higher magnitude ranges and globally valid, is critically important for any seismological or geophysical studies. In view of this, scaling relationships between magnitudes (m_b/M_s) and M_{wg} have been derived considering the entire world dataset. The m_b magnitude data for 5,24,790 events from the ISC and 3,26,106 events from the NEIC, the M_s magnitude data for 1,11,443 events from the ISC and 16,048 events from the NEIC, along with M_{wg} values for 41,810 events from the GCMT during the period 01 January 1976–31 December 2014 have been considered.

In order to compare estimation techniques of different magnitudes from different agencies (e.g., ISC, NEIC and GCMT), GOR1, GOR2 and SLR relationships have been obtained. Maximum absolute difference between ISC and NEIC body wave magnitude estimations is found to be 0.12, 0.58, and 0.234 corresponding to GOR1 (Eq. 6), GOR2 (Eq. 7) and SLR (Eq. 8), respectively. It is observed that absolute average difference between observed $m_{b,ISC}$ and $m_{b,NEIC}$ differs by 0.16 m.u where as their average difference is 0.09 m.u. A similar bias between these has also been reported by Das et al. (2011) and Utsu (2002). Present analysis indicates that m_b values obtained by ISC and NEIC are not equivalent as reported in earlier studies (e.g., Das et al. 2011).

As surface wave magnitude estimations by ISC and NEIC use the same technique, so it is expected that the magnitude determinations from these databases should be more or less equivalent (Utsu 2002; Das and Wason 2010; Das et al. 2011). The equivalence between the two M_s estimates (ISC &NEIC) has been verified for the magnitude range $2.8 \leq M_{s,NEIC} \leq 8.8$ through GOR1, GOR2 and SLR relations. Almost all these methods show M_s estimates by ISC and NEIC are equivalent and could be treated them as unified dataset. Maximum absolute difference between ISC and NEIC for Surface wave magnitude estimations is found to be 0.31, 0.01, and 0.07 corresponding to GOR1 (Eq. 9), GOR2 (Eq. 10) and SLR (Eq. 11), respectively. It is found that absolute average difference between observed $M_{S,ISC}$ and $M_{S,NEIC}$ differs by 0.098 m.u where as their average difference is −0.003 m.u.

For conversion of $m_{b,ISC}$ to M_{wg}, GOR1, GOR2 and SLR relationships have been derived using ISC and GCMT data for 36,767 events of magnitude range $4.5 \leq m_{b,ISC} \leq 6.2$ with $\eta = 0.2$. Furthermore, using three regression methodologies, slope and intercept parameters have also been obtained in the magnitude range $4.5 \leq m_{b,ISC} \leq 6.2$ for $\eta \leq 5.0$ (Fig. 4). However, previous studies for $m_{b,ISC}$ to M_w conversion were based on two methods: ISR (Inverted Standard Regression) and SLR relations between $m_{b,ISC}$ and M_w (Das et al. 2011; Scordilis, 2006). Regression coefficients computed for $m_{b,ISC}$ to M_{wg} are having lesser uncertainties in GOR1 compared to GOR2 and SLR. Correlation coefficient (Rxy) and standard deviation (RMSE) values for conversion of $m_{b,ISC}$ to M_{wg} are found to be improved in case of GOR1 compared to GOR2 and SLR (Eqs. 15–17).

Similarly, GOR1, GOR2 and SLR relationships between $m_{b,NEIC}$ and M_{wg} in the magnitude range $4.5 \leq m_{b,NEIC} \leq 6.2$ were obtained using data for 20,863 events with $\eta = 0.2$ (Fig. 3). Equations 15–20 indicate that connection between m_b and M_{wg} values is comparatively better than the connection between m_b and M_w values, and the same is already proven in Das et al. (2019).

Maximum differences between observed $m_{b,NEIC}$ and estimated M_{wg} values are found to be 0.1, 0.6 and 0.2 m.u corresponding to GOR1, GOR2 and SLR methods. The magnitude interval range ($4.5 \leq m_{b,ISC}$ /$m_{b,NEIC} \leq 6.2$) adopted in this study is primarily based on the completeness of the dataset so that more reliable relationship could be developed (Wason et al. 2012; Das et al. 2018b). However, one can extend the relationship < 4.5 for estimating indicative results.

For M_s to M_{wg} conversion, this study depicts a bilinear trend (Fig. 6a) as was also suggested by Wason et al. (2012) for M_s to M_w conversion. Therefore, the magnitude interval has been splitted into two parts: $3.1 \leq M_s \leq 6.1$ and $6.2 \leq M_s \leq 8.4$, considering the distribution is linear in these respective magnitude ranges. For conversion of M_s magnitudes to M_{wg}, GOR1, GOR2 and SLR relationships have been derived for magnitude ranges $3.1 \leq M_s \leq 6.1$ (using 19,826 events) and $6.2 \leq M_s \leq 8.4$ (using 1639 events). The observed M_s values for magnitude ranges $3.1 \leq M_s \leq 6.1$ are found to be lesser than the estimated M_{wg} by all three methods up to magnitude ≤ 5.5. The maximum observed difference between observed M_s and estimated M_{wg} by GOR1, GOR2 and SLR is found to be 0.7, 0.6 and 0.8, respectively, mainly in the lowest magnitude bin. However, these values are found to be 0.2, 0.18, and 0.23 for highest magnitude range, i.e., at magnitude 6.1. In the range of $6.2 \leq M_s \leq 8.4$, the observed M_s magnitudes are found to be lesser than the estimated M_{wg} by all three methods up to magnitude ≤ 7.4. The maximum observed differences between observed M_s and estimated M_{wg} by GOR1, GOR2 and SLR procedures are found to be 0.19, 0.25 and 0.18, respectively, mainly in the lowest magnitude range. However, these values are found to be 0.03, 0.23, and 0.13 for the highest magnitude range, i.e., at

magnitude 8.4. In order to know the regression parameters (e.g., slope and intercept) for different η values of two different types of regression relationships, a graph is presented in Fig. 7. A drastic variation in slope is observed up to $\eta = 0.8$ in case of GOR2 as compared to GOR1. However, the slope remains same for SLR method because there is no used of η for the SLR relation.

In statistical science, superiority of the regression models is generally based on the degree of uncertainty in the regression coefficients (i.e., slope, intercepts) and values of standard deviation (RMSE) and correlation coefficients (Rxy). For developing relationships between m_b or M_s and M_{wg}, GOR1 yields, in general, lesser errors in slope and intercept compared to GOR2 and SLR and provides better correlation coefficient and standard error values as compared to the other two procedures. It is important to note that GOR estimation requires η values and its (η) determination is not always appropriate, so there is a high possibility that the η value contains uncertainty. Since the GOR2 line has a higher steep than GOR1 (Figs. 4, 7), therefore, GOR2 is more sensitive with respect to η values (Das et al. 2013). Furthermore, it is also observed that, in general, the estimates given by the GOR1 procedure lie in between the estimates of GOR2 and SLR (Figs. 5, 6) for m_b and M_{wg}, M_s and M_{wg} conversions.

The regression relationships developed in this study in terms of M_{wg} based on global data are beneficial for preparing unified earthquake catalogs for any earthquake prone regime in the absence of local/regional regression relationships, as the earthquake catalog for most seismic prone areas are not homogenous in magnitude types. The GOR1 relationships developed in this study with smaller uncertainties compared to GOR2 and SLR are preferred for conversions as they transmit lower level of uncertainty in the seismic hazard assessment and seismicity studies.

Acknowledgements The article has been benefitted from funding by the Fondo Nacional de Desarrollo Cientifico y Technologico (FONDECYT) Grant Number 11200618. The authors are grateful to the reviewers for their critical reviews and constructive suggestions which helped improved technical content significantly. The authors are also grateful to the editors for their useful suggestions.

Funding Funding agency is Fondo Nacional de Desarrollo Cientifico y Technologico (FONDECYT) Grant Number 11200618.

Data and resource Earthquake data for entire world are considered during the time period 01.01.1976–31.12.2014, from ISC (International Seismological Center), U.K. (http://www.isc.ac.uk/search/Bulletin), NEIC (National Earthquake Information Center), USGS, United State of America (http://neic.usgs.gov/neis/epic/epic-global.htm) and GCMT (since 1976 now operated as Global Centroid-Moment-Tensor projectat Lamont Doherry Earth Observatory (LDEO) http://www.globalcmt.org/CMTsearch.html) earthquake data bulletins.

Declarations

Competing interests The authors acknowledge there are no conflicts of interest recorded.

References

Beresnev I (2009) The reality of the scaling law of earthquake-source spectra? J Seismol 13:433–436. https://doi.org/10.1007/s10950-008-9136-9

Bormann P, Liu R, Xu Z, Ren K, Zhang L, Wendt S (2009) First application of the new IASPEI teleseismic magnitude standards to data of the China National Seismographic Network. Bull Seismol Soc Am 99(3):1868–1891. https://doi.org/10.1785/0120080010

Carroll RI, Ruppert D (1996) The use and misuse of orthogonal regression in linear errors-in-variables models. Am Stat 50(1):1–6

Choy LG, Boatwright LJ (1995) Global patterns of radiated seismic energy and apparent stress. J Geophys Res 100(B9):18205–18228

Das R (2013) Probabilistic seismic hazard assessment for Northeast India Region. Indian Institute of Technology Roorkee, Ph.D. Thesis

Das R, Wason HR (2010) Comment on A homogeneous and complete earthquake catalog for Northeast India and the adjoining region. Seismol Res Lett 81:232–234

Das R, Wason HR, Sharma ML (2011) Global regression relations for conversion of surface wave and body wave magnitudes to moment magnitude. Nat Hazards 59:801–810

Das R, Wason HR, Sharma ML (2012) Magnitude conversion to unified moment magnitude using orthogonal regression relation. J Asian Earth Sci 50:44–51

Das R, Wason HR, Sharma ML (2013) General Orthogonal Regression Relations between body wave and moment magnitudes. Seismol Res Lett 84:219–224

Das R, Wason HR, Sharma ML (2014a) Reply to 'Comment on "Magnitude conversion problem using general orthogonal regression" by HR Wason, Ranjit Das and ML Sharma'by Paolo Gasperini and Barbara Lolli. Geophys J Int 196(1):628–631

Das R, Wason HR, Sharma ML (2014b) Unbiased estimation of moment magnitude from body-and surface-wave magnitudes. Bull Seismol Soc Am 104(4):1802–1811

Das R, Sharma ML, Wason HR (2016) Probabilistic seismic hazard assessment for Northeast India region. Pure Appl Geophys 173:2653–2670. https://doi.org/10.1007/s00024-016-1333-9

Das R, Wason HR, Sharma ML (2018a) Reply to "comments on 'Unbiased estimation of moment magnitude from body-and surface-wave magnitudes' by Ranjit Das, H.R.Wason and M.L.Sharma and 'Comparative analysis of regression methods used for seismic magnitude conversions' by P. Gasperini, B. Lolli, and S. Castellaro" by Pujol. Bull Seismol Soc Am 108(1):540–547

Das R, Wason HR, Gonzalez G, Sharma ML, Chodhury D, Roy N, Salazar P (2018b) Earthquake magnitude conversion problem. Bull Seismol Soc Am 108(4):1995–2007

Das R, Sharma ML, Wason HR, Choudhury D, Gonzalez G (2019) A seismic moment magnitude scale. Bull Seismol Soc Am 109(4):1542–1555

Ekström G, Dziewonski AM (1988) Evidence of bias in estimations of earthquake size. Nature 332(6162):319–323

Fuller WA (1987) Measurement error models. Wiley, New York

Gutenberg B (1945a) Amplitudes of P, PP and S and magnitudes of shallow earthquakes. Bull Seismol Soc Am 35:57–69

Gutenberg B (1945b) Magnitude determination for deep focus earthquakes. Bull Seismol Soc Am 35:117–130

Gutenberg B, Richter CF (1956) Magnitude and energy earthquakes. Ann Geofis 9:1–15

Hanks TC, Kanamori H (1979) A moment magnitude scale. J Geophys Res 84:2348–2350

Hutton LK, Boore DM (1987) The M_L scale in southern California. Bull Seismol Soc Am 77:2074–2094

Kagan YY (2003) Accuracy of modern global earthquake catalogs. Phys Earth Planet Inter 135:173–209

Kanamori H (1977) The energy release in great earthquakes. J Geophys Res 82:2981–2987

Kanamori H, Brodsky EE (2004) The physics of earthquakes. Rep Prog Phys 67:1429–1496. https://doi.org/10.1088/0034-4885/67/8/R03

Keir D, Stuart GW, Jackson A, Ayele A (2006) Local earthquake magnitude scale and seismicity rate for the Ethiopian rift. Bull Seismol Soc Am 96:2221–2230

Kendall MG, Stuart A (1979) The advanced theory of statistics**,** (vol 2, 4th ed), Griffin, London

Lin TL, Mittal H, Wu CF, Huang YH (2020) Spatial distribution of radiated seismic energy from earthquakes in Taiwan and surrounding regions. J Asian Earth Sci. https://doi.org/10.1016/j.jseaes.2020.104591

Madansky A (1959) The fitting of straight lines when both variables are subject to error. Am Stat Assoc J 54:173–205

Nath SK, Mandal S, Adhikari MD, Maiti SK (2017) A unified earthquake catalogue for South Asia covering the period 1900–2014. Nat Hazards 85(3):1787–1810

Purcaru G, Berckhemer H (1978) A magnitude scale for very large earthquakes. Tectonophysics 49:189–198
Richter CF (1935) An instrumental earthquake magnitude scale. Bull Seism Soc Am, 25
Richter CF (1958) Elementary seismology (W.H. Freeman, San Fransisco)
Ristau J, Rodgers G, Cassidy J (2003) Moment magnitude-local magnitude calibration for earthquakes off Canada's west coast. Bull Seismol Soc Am 93:2296–2300
Ristau J (2009) Comparison of magnitude estimates for New Zealand Earthquakes: moment magnitude, local magnitude, and teleseismic body-wave magnitude. Bull Seismol Soc Am 99:1841–1852
Utsu T (2002) Relationships between magnitude scales. In: Lee WHK, Kanamori H, Jennings PC, Kisslinger C (eds) International handbook of earthquake and engineering seismology part A. Academic Press, Amsterdam, pp 733–746
Wason HR, Das R, Sharma ML (2012) Magnitude conversion problem using general orthogonal regression. Geophys J Int 190(2):1091–1096

Authors and Affiliations

Ranjit Das[1,2] · Claudio Menesis[1] · Diego Urrutia[1]

✉ Ranjit Das
ranjit244614@gmail.com; ranjit.das@ucn.cl

[1] Department of Computer Science and Engineering, Universidad Católica del Norte, Avenida Angamos 0610, Antofagasta, Chile

[2] National Research Center for Integrated Natural Disaster Management, Santiago, Chile